Formation of self-assembled hierarchical structure on Zn doped in CuO nanoparticle using a microwave-assisted chemical precipitation approach

Bruno E
Karunya Institute of technology and Science: Karunya Institute of Technology and Sciences
Haris M
Karunya Institute of technology and Science: Karunya Institute of Technology and Sciences
https://orcid.org/0000-0001-6845-4939
Mohan A (drmohansjc@gmail.com)
Saint Joseph's College https://orcid.org/0000-0002-9589-550X
Senthilkumarb M.
Karunya Institute of technology and Science: Karunya Institute of Technology and Sciences

Research Article

Keywords: photocatalytic, CuO, microwave, Doping, hierarchical, nanoparticles

Posted Date: February 24th, 2021

DOI: https://doi.org/10.21203/rs.3.rs-184573/v1

Abstract

In the present work, CuO and $Cu_{1-x}Zn_xO$ were synthesized with the function of the Zn doping ratio by microwave-assisted chemical precipitation approach. The XRD pattern shows that the mono-phase CuO with a mono-clinical structure and no other secondary phase has been observed for the $Cu_{1-x}Zn_xO$ with different Zn ratio and confirms CuO lattice does not get destroyed by the addition of Zn. The self-assembled hierarchical flower morphology was obtained for the higher doping ratio of Zn. The Energy Dispersive Analysis of X-ray spectrum confirms the presence of Zn in the CuO lattice and the stoichiometry obtained. The optical band gap was found to be 1.78 eV for CuO nanoparticles and the values are between 1.80 and 2.29 eV for Zn doped CuO. For higher Zn doped CuO, optical band splitting was observed due to flower-like morphology. The high recombination of an electron-hole was obtained for higher doping ratio nanoparticles. These properties are needed for Photocatalytic application.

Introduction

At present, more attention is paid to metal oxide materials; in particular Copper (Cu) based metal oxides have various nanostructures, such as nanorods, nanoplates, and nanoflower. Copper oxide is a promising candidate for potential applications such as batteries [1], gas sensors [2,3], and solar cells [4], especially photo-catalysts [5]. Copper oxide is a prime material due to its abundance in nature, cost-effectiveness, thermal stability, and excellent optical response. Several synthesis methods have been reported for CuO nanostructures such as co-precipitation [1] [6] hydrothermal [7], solvothermal [8], microwave approach [2], sonochemical [3] and sol-gel methods [4]. Among these, the co-precipitation approach is a promising method for CuO nanostructure due to simple, minimal-cost, and low-temperature [9]. Also, microwave treatment is an effective process to attain nanostructures. It can provide sufficient penetrating strength into the materials and enhance the reaction during the synthesizing process. These conditions are much needed to boost the reaction process; enhance yield, increase material purity, good stoichiometry control, and well-defined size distribution [10]. To the best of our knowledge, very few papers on CuO and Zn doped CuO nanoparticles are available to synthesize using a microwave-assisted chemical precipitation approach.

CuO has a monoclinic phase and a narrow bandgap p-type multifunctional material. The value of the energy bandgap ranges between 1.2 and 1.90 eV for pure CuO [11-12]. The crystal structure and dimension play a very important role in tuning the optical response and in enhancing the catalytic properties. CuO-based metal oxides have a tunable bandgap in the lattice by host impurity ions. The optical structural, morphological, and electrical properties of the host material can be tailored by adding a metal [13-14].

Research has been performed by several investigators to understand the doping effects of metals such as Ni, Co, Zn, Cr, and Fe in CuO lattice. Among all transition metals, Zn causes more effective doping and possesses the same oxidation states [15-17]. Due to comparable ionic radii Cu2 +, zinc ion causes more efficient doping and exhibits the same oxidation state. The zinc ionic radius (0.074 nm) is nearly

equivalent to the Copper ionic radius (0.072 nm). It is very easy to substitute the Zn ions in the CuO lattice without changing crystal orientation [18]. Besides, the Zn^{2+} doping can effectively produce defects in CuO nanostructures.

The photocatalytic activity of the catalyst also strongly relies on the surface and structural properties, such as surface area, crystal composition, bandgap, and particle size [19]. The average grain size is also important and directly related to its specific surface area, which improves the efficiency of the catalyst. The large surface area, unique morphology, and crystallinity plays a vital role to enhance photocatalytic performance. CuO nanoparticle can almost satisfy the condition by adding Zn into CuO lattice and causes tailoring the properties such as structural, optical, and morphological for better photocatalytic performance.

In the present study, single-phase CuO and $Zn_xCu_{1-x}O$ nanoparticles (x=0, 0.03, 0.06, and 0.09 M) have been synthesized via a microwave-assisted precipitation method. The current work aims to investigate the effect of Zn doping on the structural, optical, and morphological properties of CuO. We investigated the impact of Zn doping, which could significantly boost photocatalytic activity.

Experimental Details

Materials

Cupric Chloride dihydrates ($CuCl_2.2H_2O$), zinc chloride ($ZnCl_2$), acetic acid (CH_3 COOH), and potassium hydroxide (KOH) were bought from Sigma Aldrich. All chemical products are used as purchased without any additional purification.

Synthesize of CuO nanoparticle

The CuO and $Cu_{1-x}Zn_xO$ nanoparticles are synthesized by microwave-assisted chemical precipitation. In a systematic synthesizing process, nanoparticles have been prepared by varying 'x' values (x = 0M (CuO), 0.03M ($Cu_{0.97}Zn_{0.03}O$), 0.06 ($Cu_{0.94}Zn_{0.06}O$) and 0.09M ($Cu_{0.91}Zn_{0.09}O$) in the $Cu_{1-x}Zn_xO$. Dihydrates cupric chloride (8.524 g) and potassium hydroxides (5.611 g) were added separately in a beaker containing 50 ml of double-distilled water. The precursor of $CuCl_2$ is stirred in magnetic stirrer for 30 minutes. Now the precursor is turned into a transparent blue solution. Next, the KOH solution is added to the $CuCl_2$ precursor drop by drop. Then, the intermediate mixture is allowed to stir overnight at room temperature and light blue precipitation has been obtained.

See formula 1 in the supplementary files.

Microwave treatment

After the process, the precursor mixture is irradiated with microwave for 180 seconds with the time interval of 10 seconds. The mixture is allowed to cool at room temperature, and now the blue color has

turned into black precipitation. Ethanol is added to the final product. The solution is further centrifuged for about 30 min and then filtered, washed with distilled water and acetone several times. The obtained product is dried in a hot air oven about 80℃ for 8 hours and calcined at 600℃ for 3 hours in a box furnace. The same procedure was adopted for the synthesis of $Cu_{1-x}Zn_xO$ nanoparticles with the addition of $ZnCl_2$ at various molar ratios. All the CuO and $Cu_{1-x}Zn_xO$ nanoparticles are characterized using powder X-ray diffraction, electron microscopy scanning, photoluminescence spectroscopy, and UV-Vis spectroscopy.

X-ray diffractions

Figure.1 illustrates the XRD pattern of $Cu_{1-x}Zn_xO$ nanoparticles with the Zn doping ratio gap using the microwave-assisted chemical precipitation approach. The diffraction planes obtained at (110), (002), (111), (02), (020), (202), (13), (310), (220), (311) and (044) correspond to the monoclinic structure of the CuO and are well-matched with the standard data (JCPDS card No. 27-0159). The same diffraction planes were obtained for all $Cu_{1-x}Zn_xO$ nanoparticles. No other significant peak is found and indicates a single monoclinic phase [20, 21].

The well-resolved peak was found at angles 35.88º and 38.35º belongs to (002), (111) planes, respectively. The decrease in intensity is directly related to the incorporation of Zn in the CuO lattice, which reduces the intensity. Changes in intensity and peak changes were observed due to the addition of the Zn^{2+} ions to the Cu^{2+} ions lattice. The structural properties have changed significantly due to a larger ion radius of Zn.

Figure.2 shows the variation of (111) and (002) with a doping ratio of Zn. This indicates the position of the peaks slightly shifted toward the lower angle of $Cu_{0.97}Zn_{0.03}O$. In contrast, the peaks for $Cu_{0.94}Zn_{0.06}O$ and $Cu_{0.91}Zn_{0.09}O$ were dramatically shifted to higher angles than $Cu_{0.97}Zn_{0.03}O$. However, the peak position is much closer to the CuO nanoparticle for ($Cu_{0.91}Zn_{0.09}O$). The higher angle shifts might be pressure stress, while tensile stress contributes to lower angle shifts. [20-22].

For CuO and Zn doped CuO nanoparticles with different Zn doping ratios, the average grain size (D), dislocation density (δ), and micro-strain (Ɛ) were estimated and it as shown in Table.1 The FWHM values are decreased for low doping of Zn doped CuO ($Cu_{0.97}Zn_{0.03}O$ and $Cu_{0.94}Zn_{0.06}O$) and increased for higher doping of Zn ($Cu_{0.91}Zn_{0.09}O$) as seen in Table.1. The average grain size was estimated using Scherrer's relations [20,21]. The grain size was estimated to be between 22 and 27 nm for CuO and Zn-doped CuO nanoparticles. The size of the grain is reduced by increasing the doping ratio compared to the CuO nanoparticles. The grain size is inversely proportional to the microstrain and dislocation density. This change is mainly due to the CuO lattice strain-induced mechanism. [23]. The variation in the diffraction plane position has shown that microstructure and grain size are dependent on the Zn doping ratio.

However, the low doping ratios of Zn induces a slight increase in the grain size of $Cu_{0.97}Zn_{0.03}O$ nanoparticles, but on a further increase of Zn doping decreases the grain size. To prevent the growth of CuO nanocrystals with Zn doping, the Zener-Pinning effect is explained. Typically, the Cu-O-Zn bond is formed at the grain boundary due to the existence of a retarding force. In this case, the retarding force is greater than the driving force for the grain growth, the grain does not grow bigger and thus the size of the grain reduces.

The lattice constants of monoclinic CuO and $Cu_{1-x}Zn_xO$ nanoparticles were estimated using the following relation and it can help to understand the substitution of radius Zn ions into Cu ions [24].

See formula 2 in the supplementary files.

Where a, b, and c are the lattice constants, d is the interplanar distance, α is the interfacial angle, and h, k, l are the Miller indices.

The calculated lattice constant values are almost identical to the standard values and are in good agreement with the previous report. The interfacial angle and unit cell volume are in good agreement with the standard data values. This indicates that no significant changes have been made due to the addition of Zn in CuO lattice. It is an interesting consequence to note that the addition of Zn will not disrupt the monoclinic crystal structure of CuO.

Morphological studies

Figure 3 shows the CuO and $Cu_{1-x}Zn_xO$ nanoparticles SEM images with a different Zn ratio. The CuO nanoparticle image shows that randomly aligned rods and cubes were identified with irregular distribution of the particles as seen in Figure.3a. This is mainly due to the anisotropic growth of the CuO monoclinic crystal and O^{2-} and Cu^{2+} ions arranged alternately in particular directions [25]. Figure 3b shows spindle-like particles for $Cu_{0.97}Zn_{0.03}O$. The hierarchical Shape with random size spherical particle is obtained for $Cu_{0.94}Zn_{0.06}O$ as seen in Figure 3c. For the $Cu_{0.91}Zn_{0.09}O$, the petals are self-assembled and cause to form the three-dimensional hierarchical flower structures as seen in Figure 3d. This may be due to the strong binding energy between individual petals due to the attractive electrostatic force. This force might be a key factor in the construction of a flower-like morphology due to self-assembled petals [31,32]. Similarly, a type of morphology has been reported for ZnO, CZTS in previous papers [27]. From the SEM study, the Zn doping ratio has a significant influence on the shape and particle size of the nanoparticle.

Elemental Analysis

Table.3 shows the energy dispersive analysis of X-ray spectra of CuO and Zn-doped CuO nanoparticles with the different Zn ratio. In the EDAX spectrum, the characteristic values were obtained only for constituent elements (Cu, Zn, and O) are observed and atomic percentages of the elements are obtained and shown in Table 3. The existence of the Zn element in Zn doped samples can be seen from the table.

The Zn/Cu ratio is estimated to be 0.0270, 0.0589 and 0.0978 for 0.03 M, 0.06M and 0.09M ratio respectively. The EDAX result confirms that the element ratio matches well with the experimental stoichiometry of $Cu_{1-x}Zn_xO$ nanoparticles and that the ratio is also almost identical [26].

Optical Properties:

Figure.4. shows the optical absorption spectra of CuO and $Cu_{1-x}Zn_xO$ nanoparticles with different Zn doping ratios. It shows that the absorption edges for all samples were identified in the UV-visible region. The absorbance edge of the $Cu_{1-x}Zn_xO$ nanoparticles was slightly shifted to a shorter wavelength (blue shift) than the CuO nanoparticles.

The bandgap energy was determined using the following equation for CuO and Zn doped CuO nanoparticles [27].

See formula 3 in the supplementary files.

Where F(R) is the function of reflectance, h**υ** is the incident photon energy, α is the absorption coefficient. The optical band gap (Eg) values are estimated from the Tauc plot by extrapolating $(\alpha h\upsilon)^2$ to photon energy. The estimated value is 1.78 eV for CuO and is in good agreement with the earlier Mohan (1.85eV) report as seen in Figure 5a. The Eg values are 1,80, and 2,08 and 2.29 eV respectively, for 3, 6, and 9 % of Zn-CuO. The energy gap values are increased by increasing the Zn doping ratio due to the quantum size effect [28,29]. The optical splitting was observed and the values for 9 % of Zn were found to be 1.90 and 2.29eV. It can be correlated with morphological properties, which can also be expressed in the XRD results.

Photocatalytic Performance

The photocatalytic activity was examined by methylene blue (MB) degradation under visible light conditions and irradiated by a halogen lamp source. In a systemic process, 20 mg of CuO is blended with 100 ml of MB solution known as a catalyst solution. The solution is being stirred in a dark condition for about 30 minutes to achieve the adsorption equilibrium. Now, after light irradiation, 3 ml of the catalyst solution was extracted from the beaker. In the same way, the process was performed for different time duration with a time interval of 15 minutes. At last, the absorbance of the supernatants is obtained at 660 nm for MB in the yellow region. Degradation efficiency ( ) is estimated using the relationship [27];

See formula 4 in the supplementary files.

Where, A_0 is the dye solution absorbance without catalyst, A_t is the dye solution absorbance in with catalyst after t.

Figure 6 shows that the photocatalytic activity of CuO and $Cu_{1-x}Zn_xO$ nanoparticles with different Zn ratios. In our case, methylene blue dye degradation with an absorption band around 660 nm with visible light irradiation is examined. Degradation of the dye was performed with the function of time and

maintained 15 minutes time interval. The degradation of the dye was observed in a dark and light condition with and without a catalyst. Degradation of MB dye is found to be 45%, 47%, 53% and 64% for CuO, 0.03M, 0.06M and 0.09M ratio of Zn respectively. The surface morphology plays a very important role in photocatalytic degradation. The hierarchical flower-like Nano petals can provide multiple reflections of the incident light. It can improve the light-harvesting and enhance the photogenerated electron holes pair sufficient to attributed photo-catalytic degradation of MB. Efficiency values are in good agreement with the previous study [30].

Figure.7 show that the room temperature emission spectra CuO and $Cu_{1-x}Zn_xO$ nanoparticles with different Zn ratio. The single emission band is obtained around at 2.84 eV for CuO and $Cu_{0.97}Zn_{0.03}O$ nanoparticles. In the case $Cu_{0.94}Zn_{0.06}O$ nanoparticle, the emission band is found at 2.67 eV, and the value slightly red-shifted than CuO nanoparticle as shown in figure 9c. The shift is related to grain size. In contrast, two emission bands were observed at 2.84eV and 2.24 eV for $Cu_{0.91}Zn_{0.09}O$ nanoparticle. The presence of two emission bands indicates the optical energy level splitting due to flower-like morphology. The PL intensity of CuO nanoparticles increased as the grain size decreases. The change in intensity provides information on the crystalline quality and recombination of the electron-hole pair. The higher intensity implies larger recombination of the electron-hole pair and higher recombination is observed for $Cu_{0.91}Zn_{0.09}O$ nanoparticles. It is mostly due to a flower-like morphology that will enhance recombination. The recombination of the electron-hole pair with the Zn doping ratio is enhanced from the PL spectra.

Conclusion

In the present work, CuO and $Cu_{1-x}Zn_xO$ nanoparticles were successfully synthesized with the function of the Zn doping ratio via microwave-assisted chemical precipitation approach. The XRD pattern reveals that the mono-phase CuO with a monoclinic structure and no other secondary phase has been observed for the Zn doped CuO nanoparticles. It also confirms that the doping of the Zn does not destroy the CuO lattice. The SEM images showed the morphological changes caused by the function of Zn doping. The flower-like morphology was obtained for $Cu_{0.91}Zn_{0.09}O$ nanoparticles. The EDAX spectra indicated the presence of Zn in the CuO lattice and the Stoichiometry corresponds to the experimental ratio. The optical band gap was found to be 1.78 for CuO nanoparticles and values are range in between 1.80 and 2.29 eV for Zn doped CuO. The result showed that the incorporation of Zn increased bandgap values. Optical band splitting was observed for higher Zn doped CuO due to flower-like morphology. The recombination of the electron-hole pair was estimated and the recombination was enhanced by Zn doping. Photocatalytic performance efficiency showed higher efficiency of 64 % for $Cu_{0.91}Zn_{0.09}O$ nanoparticles. The crystallinity, grain size, and surface morphology are important factors to be considered in the photocatalytic degradation process. It clearly shows the direct relation between Zn doping and photocatalyst performance. The result clearly shows that the structural, optical, and morphological and photocatalytic performance of Zn doping has been enhanced. We can tailor the optical band gap by Zn doping, which causes morphological change and leads to improved catalyst performance. From the above finding, the Zn is a very good substitution metal in CuO lattice and evident here.

Reference

1. Li X, Guo W, Liu Y, He W, Xiao Z (2014) Spinel LiNi0.5- Mn1.5O4 as superior electrode materials for lithium-ion batteries: Ionic liquid assisted synthesis and the effect of CuO coating. Electrochimica Acta 116:278
2. Lee J, Katoch A, Kim J, Kim S (2016) Effect of Au nanoparticle size on the gas-sensing performance of p-CuO nanowires. Sens Actuators B Chem 222:307
3. Etefagh R, Azhir E, Shahtahmasebi N (2013) Synthesis of CuO nanoparticles and fabrication of nanostructural layer biosensors for detecting Aspergillus niger fungi. Sci Iran F 20(3):1055.
4. Siddiqui H, Qureshi MS, Haque FZ (2016) Valuation of copper oxide (CuO) nanoflakes for its suitability as an absorbing material in solar cells fabrication. Optik 127:3713
5. Sharma A, Varshney M, Kyun HT, Chae KH, Shin HJ (2015) X-ray absorption spectroscopy study and photocatalyst application of CuO and Cu0.9Ti0.1O nanoparticles. Curr App Phys 15:1148.
6. Fuku X, Kaviyarasu K, Matinise M, Maaza M (2016) Punicalagin green functionalized $Cu/Cu_2O/ZnO/CuO$ nanocomposite for potential electrochemical transducer and catalyst. Nanoscale Res Lett 11:386
7. El-Trass A, Shamy HE, Mehasse IE, Kemary ME (2012) CuO nanoparticles: synthesis, characterization, optical properties and interaction with amino acids. Appl Surf Sci 258:2997.
8. Jiang T, Wang Y, Meng D, Wu X, Wang J, Chen J (2014), Controllable fabrication of CuO nanostructure by hydrothermal method and its properties. Appl Surf Sci 311:602
9. Prakash, C. Tirupathi, Synthesis and Characterization of Pure and Rare-Earth Metal Gd Doped SnO_2-CuO Nanoparticles by Co-Precipitation Method, Journal of Nanoscience and Technology, Volume 4,Issue 5,2018 Pages 478-482.
10. Kumar MA, Kumaran SM (2015) Effect of Ni doping on electrical, photoluminescence and magnetic behaviour of Cu doped ZnO nanoparticles. J Lumin 162:97.
11. Jiang T, Wang Y, Meng D, Wu X, Wang J, Chen J (2014) Controllable fabrication of CuO nanostructure by hydrothermal method and its properties. Appl Surf Sci 311:602.
12. Arun Kumar D, Francis P. Xavier and Merline Shyla J 2012 Archives of Applied Science Research 4 (5) 2174.
13. Iqbal, T. Jan, S.U. Hassan, I. Ahmed, Q. Mansoor, M. Umair Ali, F. Abbas, M. Ismail, Facile synthesis of Zn doped CuO hierarchical nanostructures: Structural, optical and antibacterial properties, AIP Advs. 5 (2015) 01-09.
14. Jayaprakash, N. Srinivasan, P. Chandrasekaran, E. K. Girija, Synthesis and characterization of cluster of grapes like pure and Zinc doped CuO nanoparticles by sol–gel method, Spectrochim. Acta Part A: Mol. Biomol. Spect. 136 (2015) 1804- 1806.
15. Li X, Guo W, Liu Y, He W, Xiao Z (2014) Spinel LiNi0.5- Mn1.5O4 as superior electrode materials for lithium-ion batteries: Ionic liquid assisted synthesis and the effect of CuO coating. Electrochimica

Acta 116:278.

16. Lee J, Katoch A, Kim J, Kim S (2016) Effect of Au nanoparticle size on the gas-sensing performance of p-CuO nanowires. Sens Actuators B Chem 222:307.
17. Siddiqui H, Qureshi MS, Haque FZ (2016) Valuation of copper oxide (CuO) nanoflakes for its suitability as an absorbing material in solar cells fabrication, Optik 127:3713.
18. Kumar MA, Kumaran SM (2015) Effect of Ni doping on electrical, photoluminescence and magnetic behaviour of Cu doped ZnO nanoparticles. J Lumin 162:97.
19. Ahmed S (2011) Impact of operating conditions and recent developments in heterogeneous photocatalytic water purification process. Crit Rev Environ Sci Technol 42(6):601–675.
20. O. Yathisha and Y. Arthoba Nayaka, Structural, optical and electrical properties of zinc incorporated copper oxide nanoparticles: doping effect of Zn, Journal of Materials Science volume 53, pages678–691(2018).
21. O. Yathisha, Y. Arthoba Nayaka, P. Manjunatha, H.T. Purushothama, M.M. Vinay, K.V. Basavarajappa, Study on the effect of Zn2+ doping on optical and electrical properties of CuO nanoparticles, Physica E: Low-dimensional Systems and Nanostructures Volume 108, April 2019, Pages 257-268.
22. Ansari SA, Nisar A, Fatma B, Khan W, Naqvi AH (2012) Investigation on structural, optical and dielectric properties of Co doped ZnO nanoparticles synthesized by gel-combustion route. Mater Sci Eng B 177:429
23. Vaseem M, Umar A, Kim SH, Hahn YB (2008) Low-Temperaturesynthesis of flower shaped CuO nanostructures by solution process: formation mechanism and structural properties, J Phys Chem C 112:5735.
24. Yildirim OA, Durucan C (2016) Room temperature synthesis of Cu incorporated ZnO nanoparticles with room temperature ferromagnetic activity: structural, optical and magnetic characterization. Ceram Int 42:3232.
25. Ahsanulhaq Q, Kim JH, Lee JS, Hahn HB (2010) Electrical and gas sensing properties of ZnO nanorod arrays directly grown on a four-probe electrode system. Electrochem Commun 12:477.
26. Muthukumaran S, Gopalakrishnan R (2012) Structural, FTIR and photoluminescence studies of Cu doped ZnO nanopowders by co-precipitation method. Opt Mater 34:1949.
27. Sheebha, VanisreeVenugopal, JudyJames, V.Maheskumar, A.Sakunthala and B.Vidhya, Comparative studies on hierarchical flower like Cu2XSnS4[X= Zn, Ni, Mn & Co] quaternary semiconductor for electrocatalytic and photocatalytic applications, International Journal of Hydrogen Energy, Volume 45, Issue 15, 18 March 2020, 8139-8150.
28. Hassan MM, Khan W, Azam A, Naqvi AH (2015) Influence of Cr incorporation on structural, dielectric and optical properties of ZnO nanoparticles. J Ind Eng Chem 21:290.
29. Yathisha RO, Arthoba Nayaka Y, Vidyasagar CC (2016), Microwave combustion synthesis of hexagonal prism shaped ZnO nanoparticles and effect of Cr on structural, optical and electrical properties of ZnO nanoparticles. Mater Chem Phys 181:174.

30. Phaltane SA, Vanalakar SA, Bhat TS, Patil PS, Sartale SD, Kadam LD. Photocatalytic degradation of methylene blue by hydrothermally synthesized CZTS nanoparticles. J Mater Sci Mater Electron 2017;28:8186-91.
31. Mageshwari • R. Sathyamoorthy, Organic free synthesis of flower-like hierarchical CuO microspheres by reflux condensation approach, Appl Nanosci (2013) 3:161–166.
32. Javed Iqbal, , Tariq Jan, , Sibt Ul-Hassan, Ishaq Ahmed, Qaisar Mansoor, M. Umair Ali, Fazal Abbas, and Muhammad Ismail, Facile synthesis of Zn doped CuO hierarchical nanostructures: Structural, optical and antibacterial properties, AIP Advances **5**, 127112 (2015).

Tables

Due to technical limitations, tables are available as a download in the supplementary files.

Figures

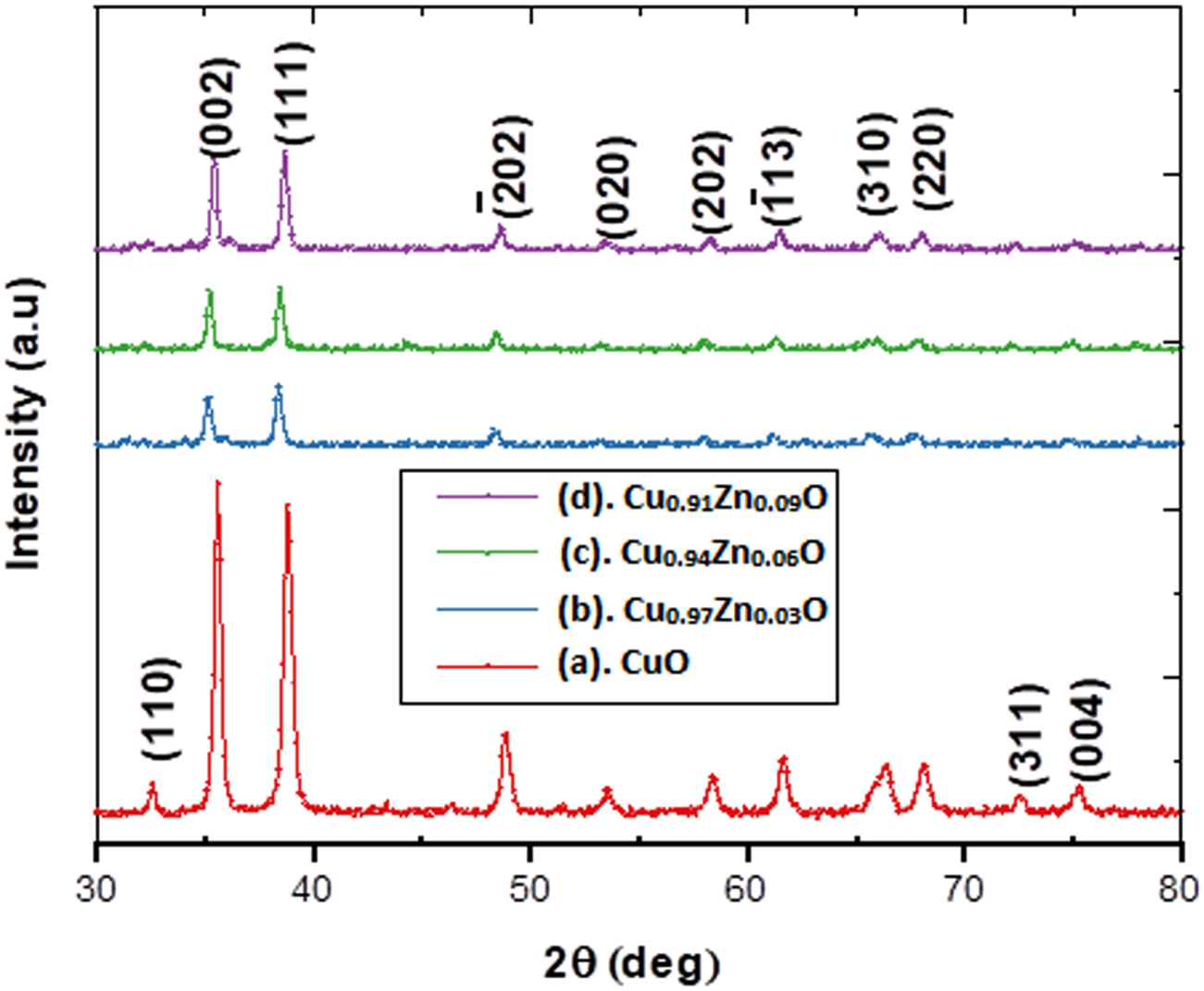

Figure 1

XRD pattern of CuO and Cu1-xZnxO, (a). CuO, (b). Cu0.97Zn0.03O, (c). Cu0.94Zn0.06O and (d). Cu0.91Zn0.09O.

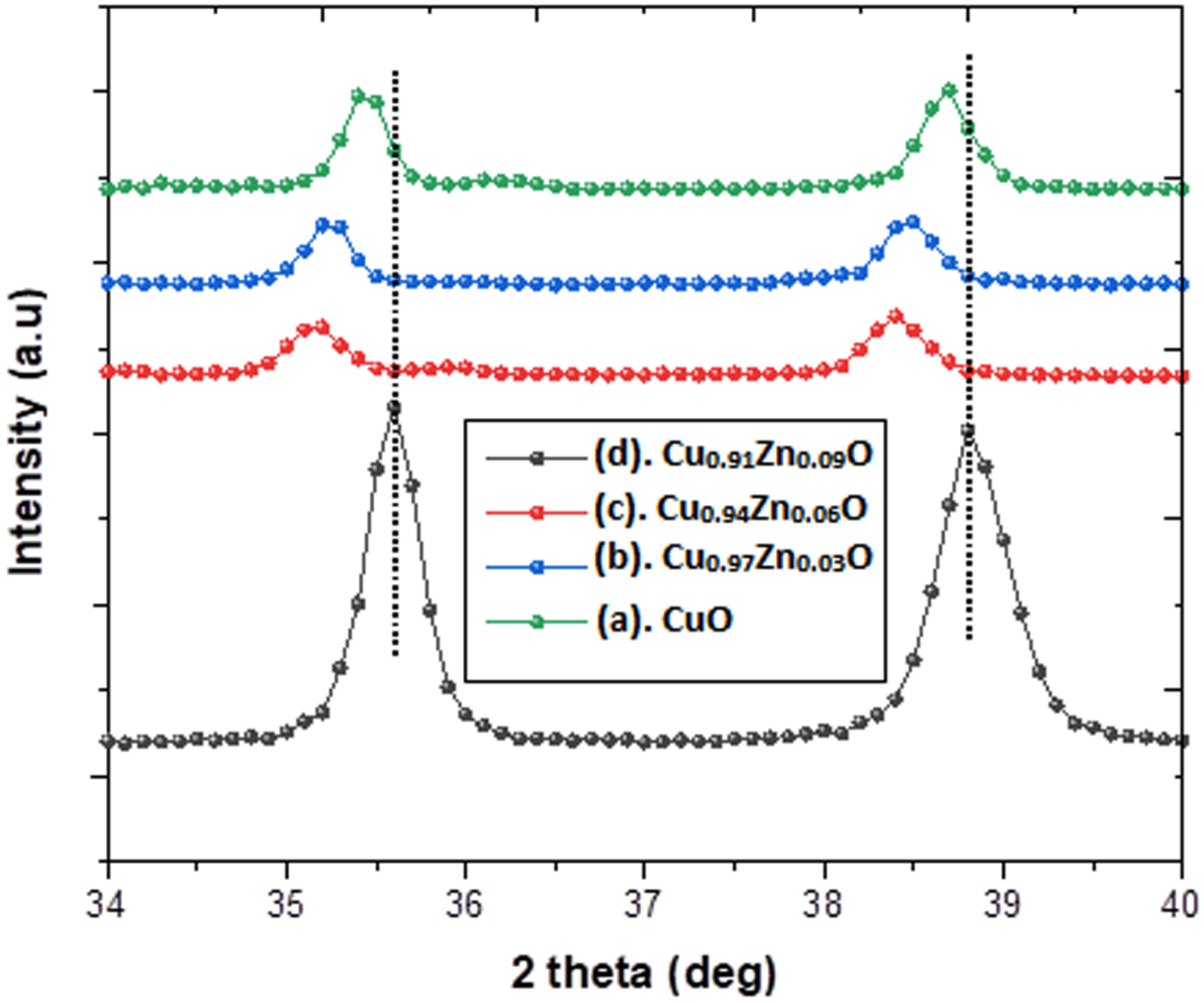

Figure 2

Variation of (002) and (111) with the function Zn doping, (a). CuO, (b). Cu0.97Zn0.03O, (c). Cu0.94Zn0.06O and (d). Cu0.91Zn0.09O.

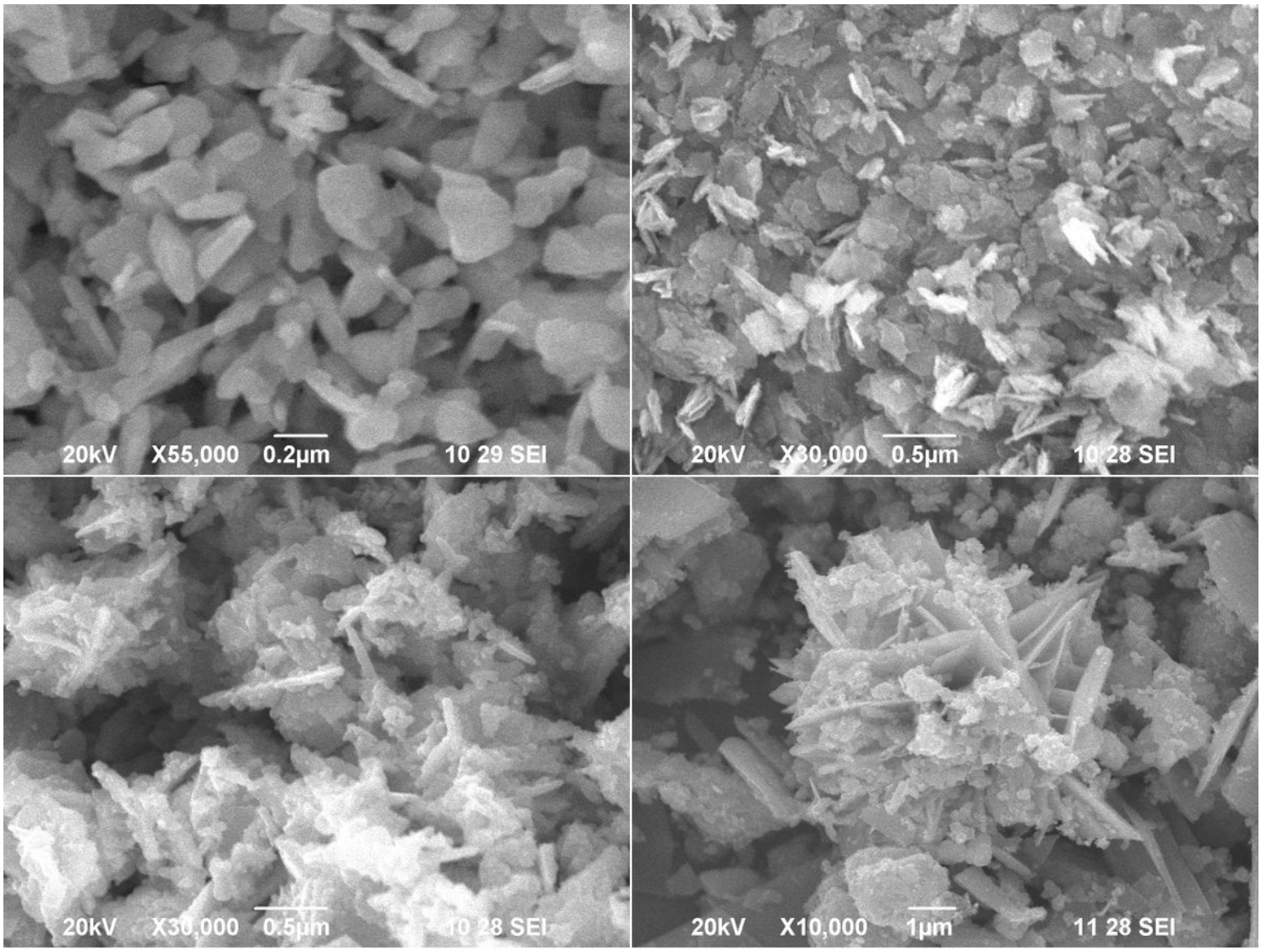

Figure 3

Scanning electron microscope images of CuO and Cu1-xZnxO nanoparticles, (a). CuO, (b). Cu0.97Zn0.03O, (c). Cu0.94Zn0.06O and (d). Cu0.91Zn0.09O.

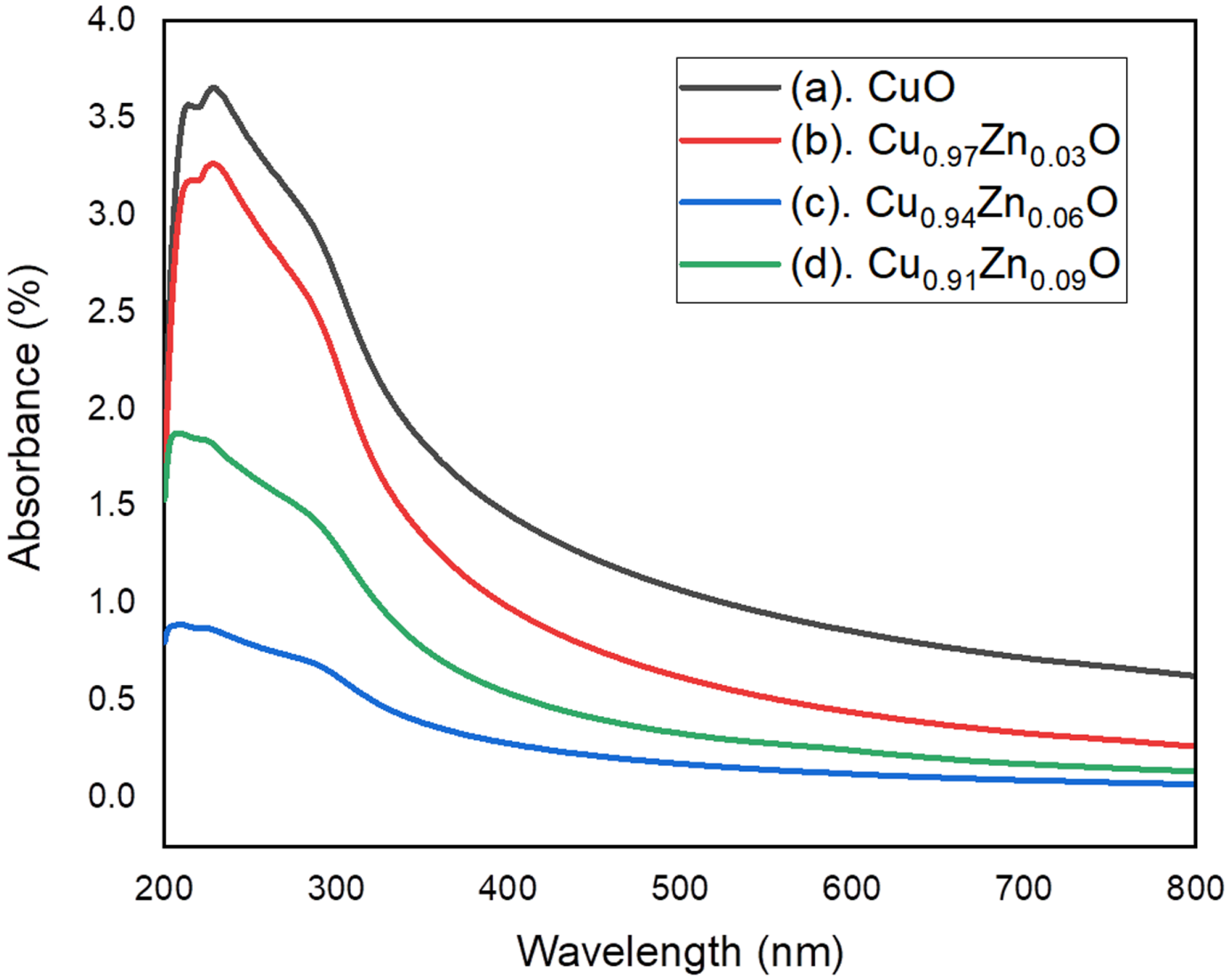

Figure 4

Optical absorption spectra of CuO and Cu1-xZnxO nanoparticles, (a). CuO, (b). Cu0.97Zn0.03O, (c). Cu0.94Zn0.06O and (d). Cu0.91Zn0.09O.

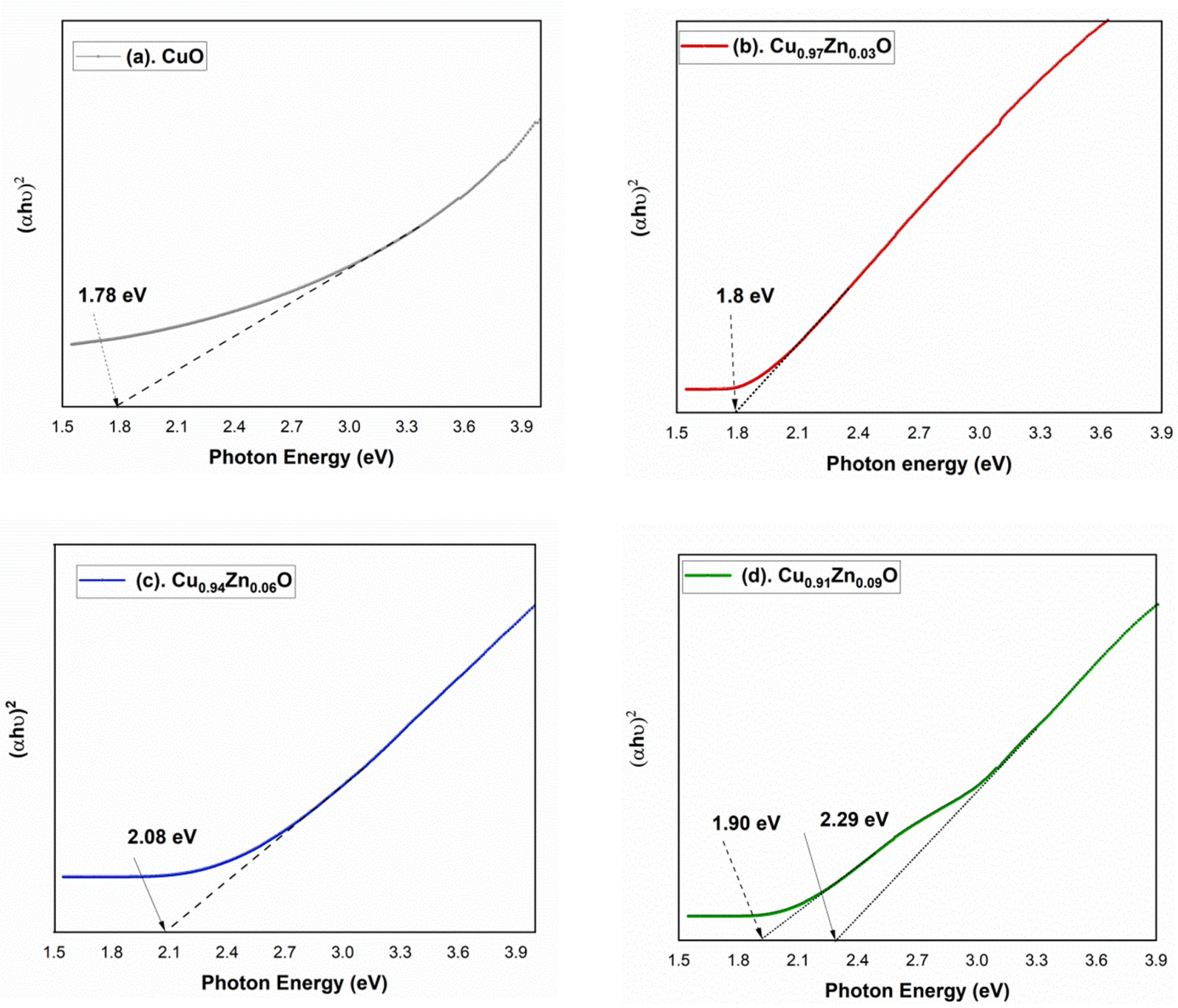

Figure 5

Optical Bandgap of CuO and Cu1-xZnxO nanoparticles, (a). CuO, (b). Cu0.97Zn0.03O, (c). Cu0.94Zn0.06O and (d). Cu0.91Zn0.09O.

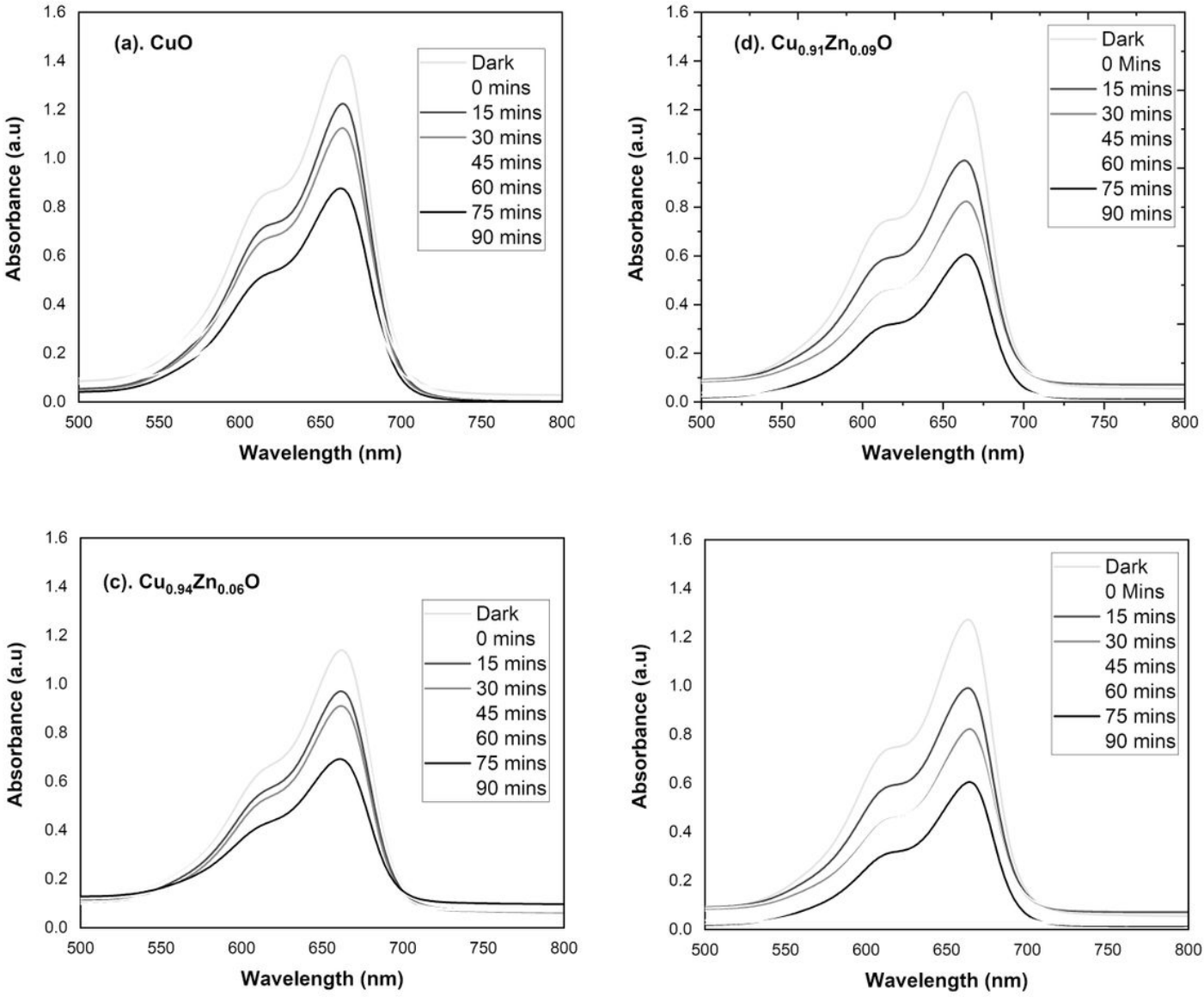

Figure 6

Photocatalytic activity of CuO and Cu1-xZnxO nanoparticles, (a). CuO, (b). Cu0.97Zn0.03O, (c). Cu0.94Zn0.06O and (d). Cu0.91Zn0.09O.

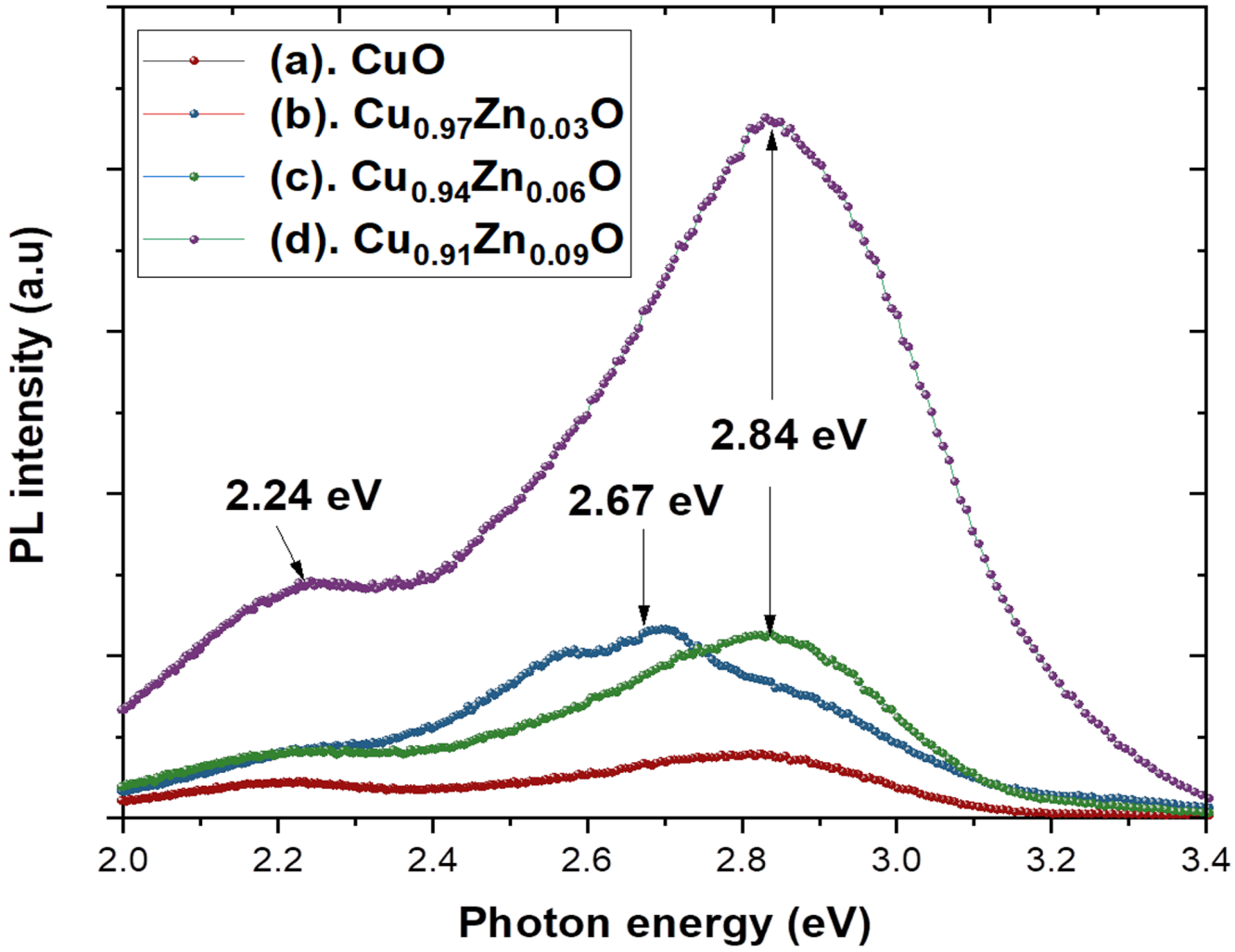

Figure 7

Room temperature PL emission Spectra of CuO and Cu1-xZnxO, (a). CuO, (b). Cu0.97Zn0.03O, (c). Cu0.94Zn0.06O and (d). Cu0.91Zn0.09O.

Supplementary Files

This is a list of supplementary files associated with this preprint. Click to download.

- Tables.docx
- formulas.docx